J Neurophysiol 125: 282–295, 2021.
First published December 2, 2020; doi:10.1152/jn.00304.2020

american physiological society

JNP JOURNAL OF NEUROPHYSIOLOGY

RESEARCH ARTICLE

Sensory Processing

Dependence of the stimulus-driven microsaccade rate signature in rhesus macaque monkeys on visual stimulus size and polarity

Tatiana Malevich,[1,2,3] Antimo Buonocore,[1,2] and Ziad M. Hafed[1,2]

[1]*Werner Reichardt Centre for Integrative Neuroscience, Tuebingen University, Tuebingen, Germany;* [2]*Hertie Institute for Clinical Brain Research, Tuebingen University, Tuebingen, Germany; and* [3]*Graduate School of Neural and Behavioural Sciences, International Max-Planck Research School, Tuebingen University, Tuebingen, Germany*

Abstract

Microsaccades have a steady rate of occurrence during maintained gaze fixation, which gets transiently modulated by abrupt sensory stimuli. Such modulation, characterized by a rapid reduction in microsaccade frequency followed by a stronger rebound phase of high microsaccade rate, is often described as the microsaccadic rate signature, owing to its stereotyped nature. Here, we investigated the impacts of stimulus polarity (luminance increments or luminance decrements relative to background luminance) and size on the microsaccadic rate signature. We presented brief, behaviorally irrelevant visual flashes consisting of large or small, white or black stimuli over an otherwise gray image background. Both large and small stimuli caused robust early microsaccadic inhibition, but postinhibition microsaccade rate rebound was significantly delayed and weakened for large stimuli when compared with small ones. Critically, small black stimuli were associated with stronger modulations in the microsaccade rate signature than small white stimuli, particularly in the postinhibition rebound phase, and black stimuli also amplified the incidence of early stimulus-directed microsaccades. Our results demonstrate that the microsaccadic rate signature is sensitive to stimulus size and polarity, and they point to dissociable neural mechanisms underlying early microsaccadic inhibition after stimulus onset and later microsaccadic rate rebound at longer times thereafter. These results also demonstrate early access of oculomotor control circuitry to diverse sensory representations, particularly for momentarily inhibiting saccade generation with short latencies.

NEW & NOTEWORTHY Microsaccade rate is transiently reduced after sudden stimulus onsets, and then strongly rebounds before returning to baseline. We explored the influence of stimulus polarity (black vs. white) and size on this "rate signature." Large stimuli caused more muted microsaccadic rebound than small ones, and microsaccadic rebound was also differentially affected by black versus white stimuli, particularly with small stimuli. These results suggest dissociated neural mechanisms for microsaccadic inhibition and rebound in the microsaccadic rate signature.

cueing; fixational eye movements; microsaccades; on and off responses; saccadic inhibition

INTRODUCTION

Microsaccades occur occasionally during steady-state gaze fixation. When an unexpected stimulus onset occurs under such steady-state conditions, as is the case in a variety of behavioral experiments requiring maintained fixation (1), stereotyped changes in microsaccade likelihood (and other properties) take place. Specifically, microsaccade likelihood, or rate per second, abruptly decreases shortly after stimulus onset, remains near zero for a brief period of time, and then momentarily rebounds to higher rates than before stimulus onset (2–11). This pattern has been termed the "microsaccadic rate signature" (4, 5, 8, 12, 13), owing to its highly repeatable nature across paradigms, and it is also related to the more general phenomenon of saccadic inhibition (14–21).

The neural mechanisms behind the microsaccadic rate signature, and saccadic inhibition in general, are still being investigated. Neurophysiological perturbation studies in the superior colliculus (SC), frontal eye fields (FEF), and primary visual cortex (V1) provide initial informative steps toward

Correspondence: T. Malevich (tatiana.malevich@cin.uni-tuebingen.de).
Submitted 26 May 2020 / Revised 18 November 2020 / Accepted 2 December 2020

clarifying these mechanisms. First, using a paradigm involving peripheral stimulus onsets, Hafed et al. (22) demonstrated that monkeys exhibit the same microsaccadic rate signature as humans. These effects persisted even after thousands of trials performed by the same animals in the same tasks, confirming the systematic nature of the effects. These authors then exploited the observation that monkeys exhibit the same phenomenon as humans to perform invasive neurophysiology; they reversibly inactivated portions of the SC topographic map representing the locations of the appearing peripheral stimuli (23). The microsaccadic rate signature was virtually unaltered, whereas microsaccade directions were significantly redistributed (23), consistent with a dissociation between the rate signature and stimulus-induced microsaccade direction oscillations (3, 5, 24). In follow-up work, Peel et al. (7) extended these results by reversibly inactivating the FEF. They found that the early inhibition was again unaltered, but, critically, the rebound phase of the microsaccadic rate signature was affected; there were fewer postinhibition microsaccades than without FEF inactivation. In V1, preliminary results show that lesions affected microsaccades, but the early inhibition after stimulus onset still appeared to be present (25). Together with computational modeling (5, 24), all of these initial results suggest that there may be different components associated with the rate signature (e.g., inhibition vs. rebound) that are mediated by distinct neural circuits; the early inhibition is clearly distinct from the later rebound that seems to particularly require frontal cortical control.

That said, the microsaccadic rate signature in its entirety must still be related to early sensory responses, as the inhibition phase starts with very short latencies from stimulus onset (~60–70 ms in monkeys) (9, 22, 26). It is, therefore, worthwhile to explore the effects of stimulus properties on subsequent microsaccadic modulations. For example, Rolfs et al. (8, 11) investigated the impacts of luminance and color contrast, as well as auditory stimulation, on microsaccadic inhibition. Similarly, contrast sensitivity was related to the microsaccadic rate signature in other recent studies (2, 13). In all of these investigations, the general finding was that the strength of both inhibition and subsequent rebound increases with increasing stimulus strength. This suggests that expected sensory neuron properties (e.g., increased neural activity with increased stimulus contrast) must act rapidly on the oculomotor system to mediate inhibition and, potentially, also influence subsequent rate rebounds. Interestingly, the path to these primarily "sensory" studies was only possible through earlier investigations of the links between microsaccades and cognitive processes of attention (4, 27). In that regard, it was the work of Laubrock et al. (6) that helped to jumpstart looking at the impacts of exogenous and endogenous attentional cues on microsaccade rate and how such rate might be dissociated from the time course of microsaccade directions. The net result is, as alluded to earlier, a class of models incorporating both sensory and top-down signals in explaining the temporal dynamics of microsaccades after a variety of sensory and cognitive events (5, 24, 28, 29).

Here, we add to the existing descriptive studies about the microsaccadic rate signature by documenting new evidence that visual stimulus polarity matters. We presented localized as well as diffuse visual flashes that were either white or black, relative to an otherwise gray background. We found that black localized stimuli were particularly effective in modulating the microsaccadic rate signature when compared with white stimuli, especially in the rebound phase, even when the white stimuli had higher contrast relative to the background. Besides helping to clarify the properties of sensory pathways affecting the microsaccadic rate signature, our results are additionally important because of the above-mentioned links to spatial attention shifts (1, 4, 9, 24, 27, 30, 31). Despite accumulated evidence on differential effects of stimulus contrast on both so-called facilitatory and inhibitory cueing effects and on reaction times in general (32–35), the question of whether and to what extent stimulus polarity itself affects cueing effects has, to our knowledge, not been explicitly addressed. Because microsaccades can potentially play an integral role in cognitive processes such as covert attention (1, 9, 24, 27, 30, 31), we believe that knowing more about the stimulus conditions (and pathways) that might maximize or minimize the likelihood of microsaccades in a given paradigm would be useful in cognitive and systems neuroscience in general.

METHODS

Ethics Approvals

All monkey experiments were approved by ethics committees at the Regierungspräsidium Tübingen. The experiments were in line with the European Union directives and the German laws governing animal research.

Laboratory Setups

Monkey experiments were performed in the same laboratory environment as that described recently (26, 36, 37). For one monkey's data, the display system was updated to a newer, faster, and brighter device, as detailed in the next paragraph. Also, a subset of the data (from the full-screen flash condition described in *Monkey Behavioral Tasks*, and only from monkeys M and A) were analyzed in brief in Malevich et al. (26), to compare the timing of microsaccadic inhibition to the novel ocular position drift phenomenon described in that study. However, the present study describes new analyses and comparisons to different stimulus conditions that are not reported on in the previous study.

For two monkeys (M and A), stimuli were presented on a cathode-ray-tube (CRT) display running at 120 Hz refresh rate. The display was γ-corrected (linearized) and the stimuli were grayscale. For monkey F, the display was updated to a high-speed LCD device running at 138 Hz (AOC AG273QX 27″). Background and stimulus luminance values are described in the *Monkey Behavioral Tasks* section. Stimulus control was achieved using the Psychophysics Toolbox (38–40). The toolbox received display update commands from a controller device and it sent back confirmation of display updates. The controller device consisted of a real-time computer from National Instruments, controlling all aspects of data acquisition (including digitization of eye-position signals) and reward of the animals (in addition to display control). The real-time computer communicated with the Psychophysics Toolbox, using direct Ethernet connections and universal data packet (UDP) protocols (41).

Animal Preparation

We collected behavioral data from three adult, male rhesus macaques (*Macaca Mulatta*). Monkeys M and A (aged 7 yr and weighing 9–10 kg) were implanted with a scleral search coil in one eye to allow measuring eye movements (sampled at 1 KHz), using the electromagnetic induction technique (42, 43). For monkey F (aged 11 yr and weighing 14 kg), we detected microsaccades from eye movement samples recorded by a video-based eye tracker (EyeLink1000; desktop mount; 1 KHz sampling rate). The monkeys were also implanted with a head holder to stabilize their head during the experiments, with details on all implant surgeries provided earlier (37, 41). The monkeys were part of a larger neurophysiology project beyond the scope of the current manuscript.

Monkey Behavioral Tasks

For monkeys M and A, fixation was maintained on a small square spot of ~5 × 5 min arc dimensions. The spot was white (86 cd/m^2) and drawn over a uniform gray background (29.7 cd/m^2) in the rest of the display. The display subtended approximately ±15° horizontally and ±11° vertically relative to central fixation, and the rest of the laboratory setup beyond the display was dark. For monkey F, the newer LCD display subtended approximately ±22° horizontally and ±13° vertically, and the gray background had a luminance of 36.5 cd/m^2. The white fixation spot was 11 × 12 min arc in size and its luminance was 132.5 cd/m^2. After ~550–1,800 ms of initial fixation, a single-frame (~8 ms for monkeys M and A and ~7 ms for monkey F) flash occurred to modulate the microsaccadic rate signature. In different conditions, the flash could be either a full-screen flash, for which monkey M and A microsaccades were only partially analyzed in Malevich et al. (26), or a localized flash (not previously analyzed in all three monkeys). The latter was a square of 1 × 1° dimensions centered on either 2.1° to the right or left of the fixation spot. On randomly interleaved control trials, the flash was sham (i.e., no flash was presented) and nothing happened on the display until trial end. Each session, therefore, had four equally likely conditions: control, small flash to the right, small flash to the left, or full-screen flash. Approximately 100–1,400 ms after flash onset, the fixation spot disappeared, and the monkeys were rewarded for maintaining gaze fixation at the fixation spot throughout the trial. Note that this paradigm is the fixation variant of the paradigm that we used earlier during smooth pursuit eye movements generated by the same monkeys (36). Also note that the equal likelihood of all four conditions across trials (e.g., see Fig. 1 in RESULTS) means that our observations of differential effects of the different flash types on microsaccadic rate modulations are unlikely to reflect known oddball effects (10).

In one block of sessions, the stimuli used could be white flashes of the same luminance as the fixation spot (5,167 trials analyzed from monkey M, 3,104 trials analyzed from monkey A, and 2,196 trials from monkey F). In another block, the stimuli were all black flashes, but the fixation spot was still white (1,513 trials analyzed from monkey M, 1,818 trials analyzed from monkey A, and 2,215 trials from monkey F). Because we hypothesized that black flashes would have stronger influences, in general, than white flashes, motivated by earlier evidence in visual perception studies (44–46), we aimed to ensure that such stronger influences would be independent of stimulus contrast relative to the background. That is, because stimulus contrast can affect the microsaccadic rate signature (as detailed in INTRODUCTION), we avoided a potential confound of stimulus contrast by having our background gray luminance level being closer to black than to white. Thus, relative to the background luminance, the contrast of black flashes was lower than that of white flashes. Yet, as we report in RESULTS, black flashes often still had significantly stronger impacts on the microsaccadic rate signature, especially with the localized stimuli.

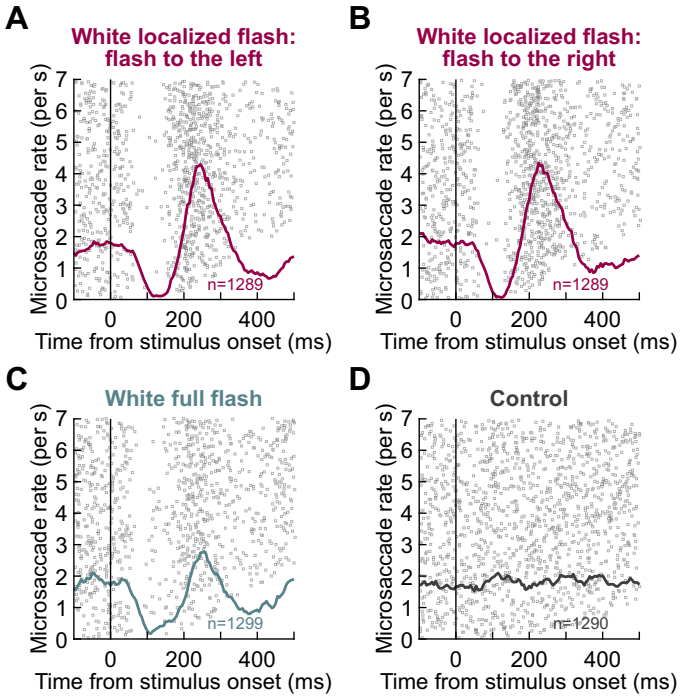

Figure 1. Microsaccadic modulations after brief, behaviorally irrelevant flashes. *A* and *B:* each row of dots is a trial, and each dot is the time of a microsaccade onset in the trial. The shown trials were all from monkey M with a white localized flash to the left (*A*) or right (*B*) of fixation. Also, the trials were sorted by increasing duration from bottom to top; therefore blanks near the bottom of the raster merely indicate that trials had ended and we stopped measuring microsaccades (METHODS). As can be seen, there was robust microsaccadic inhibition shortly after flash onset, followed by a strong rebound. *C*: similar analyses for the same monkey but now when diffuse, full-screen flashes were presented. Similar microsaccadic inhibition occurred, but the rebound in microsaccade incidence after the inhibition was weaker than with the localized flashes. *D*: microsaccades in a control condition (sham flashes; METHODS) were unmodulated. In all panels, the continuous curve shows the estimate of microsaccade rate (movements per second) from the underlying microsaccade rasters, as described in METHODS. Trial numbers per condition are also indicated in each panel.

Behavioral Analyses

We detected microsaccades using established methods reported elsewhere (41, 47). Both methods rely on a mathematical differential (i.e., speed) or more (i.e., acceleration) of the digitized eye position signals acquired by our systems, with specific parameters for the classification of saccadic

events depending on the specific signal noise levels in the digitized signals. We manually inspected each trial to correct for false alarms or misses by the automatic algorithms, which were rare. We also marked blinks or noise artifacts for later removal. In scleral eye coil data, blinks are easily discernible due to well-known blink-associated changes in eye position. In video-based eye tracking data, blinks occlude the tracked pupil and corneal reflection, resulting in no measurements.

We estimated microsaccade rate as a function of time from stimulus onset, using similar procedures to those we used earlier (3, 22, 26). Briefly, for any time window of 50-ms duration and in any one trial, we counted how many microsaccades occurred within this window (typically 0 or 1). This gave us an estimate of instantaneous rate within such a window (i.e., expected number of microsaccades per rectangular time window, divided by 50-ms window duration). We then moved this rectangular window in steps of 5 ms to obtain full time courses. The mean microsaccade rate curve across all trials of a given condition was then obtained by averaging the individual trial rate curves, and we obtained the standard error of the mean as an estimate of the dispersion of the across-trial measurements. Since some trials ended before 500 ms after flash onset (see *Monkey Behavioral Tasks*), the across-trial average and standard error estimates that we obtained for any given time bin were restricted to only those individual trials that had data in this time bin; this was a majority of trials anyway (e.g., see Fig. 1). Also, because of the window duration and step size, the time courses were effectively low-pass filtered (smoothed) estimates of microsaccade rate (48); that is, the method is effectively a moving average with a rectangular window. This kind of smoothing is inevitable when converting a discrete point process (microsaccade onset times) into a rate estimate (8). We did not analyze potential higher frequency oscillations in microsaccade rate time courses. These tend to come later after the rebound phase anyway (24). We also confirmed that prestimulus baseline microsaccade rate in a given monkey was similar in the separate blocks of white and black flashes, therefore allowing us to compare and contrast polarity effects on the rate signature after flash onsets.

With localized flashes, we also considered microsaccade rate time courses independently for specific subsets of microsaccade directions. We specifically considered microsaccades that were either congruent or incongruent with flash location (meaning that we pooled right-flash and left-flash conditions together for these analyses). Congruent microsaccades were defined as those movements with a horizontal component in the direction of the flash. Incongruent microsaccades were defined as movements with a horizontal component opposite the flash location. Our past work shows that this categorization based on only the horizontal component of microsaccades is sufficient, especially since microsaccade vector directions after localized flashes are anyway highly systematically associated with the flash direction (5, 9). In related analyses, we also plotted direction distributions independently of microsaccade rate. Here, for every time bin relative to stimulus onset, we calculated the fraction of microsaccades occurring within this time bin that were congruent with flash location. This gave us a time course of direction distributions for all microsaccades that did occur (whether during the inhibition or rebound phases of the microsaccadic rate signature).

Statistical Analyses

All figures show error bars, which encompassed the standard error bounds around any given curve. The figure legends explain the meaning of the shown error bars.

To statistically test the difference in the microsaccadic rate signature between conditions, we used nonparametric permutation tests with cluster-based correction for multiple comparisons (49), as we also described in detail in Bellet et al. and Idrees et al. (48, 50). First, for each time point (a bin) within an interval from −100 ms till +500 ms relative to stimulus onset, we compared two given conditions (e.g., localized vs. full-screen flashes) by calculating the mean difference in their microsaccade rate. To obtain the null experimental distribution, we collected the trials from both conditions into a single set and, while maintaining the initial ratio of numbers of trials in each of the conditions, we randomly permuted their labels; we repeated this procedure 1,000 times and recalculated the test statistic (i.e., the difference in rate curves between the two conditions) on each iteration. Second, we selected the bins of the original data whose test statistics were either below the 2.5th percentile or above the 97.5th percentile of the permutation distribution (i.e., significant within the 95% confidence level). For adjacent time bins having significant differences (i.e., for clusters of significance), we classified them into negative and positive clusters based on the sign of the difference in rate curves between the two conditions (i.e., clusters had either a negative or positive difference between the two compared microsaccade rate curves). We also repeated this procedure for each random permutation iteration by testing it against all other 999 random permutation iterations. This latter step gave us potential clusters of significance (positive or negative) that could arise by chance in the random permutations. Third, for both the observed and permuted data, we calculated the cluster-level summary statistic; this was defined as the sum of all absolute mean differences in any given potentially "significant" cluster. After that, we computed the Monte Carlo P values of the original data's clusters by assessing the probability of getting clusters with larger or equal cluster-level statistics under the null distribution (i.e., by taking the count of null data clusters with test statistics equal to or larger than the test statistic of any given original data cluster and dividing this count by the number of permutations that we used). Note that these P values were essentially just counts of which clusters were consistent with the null distribution. Therefore, a P value of 0 reported in RESULTS indicates that none of the clusters of the null distribution had larger or equal cluster-level statistics than the real experimental data.

When testing either the localized or full-screen flash conditions against the control condition, the test was two-sided (i.e., looking for either positive or negative clusters) to avoid mutual masking of the expected inhibition and rebound effects. In this case, positive and negative clusters (i.e., clusters with positive and negative mean rate differences, respectively) in the experimental data were compared with positive and negative clusters in the permuted data, respectively; the clusters whose P values exceeded the critical α

level of 0.025 were considered as significant. All other comparisons were done with a one-tailed test, whereby the clusters were compared in their absolute value regardless of their sign; the critical α level was set to 0.05 in this case.

When comparing magnitudes of the effects in different phases of the microsaccadic rate signature across conditions, we ran additional nonparametric permutation tests on the differences in minimum microsaccade rates during the inhibition phase or differences in peak microsaccade rates in the rebound phase, as well as in their latencies. To that end, based on the observations in each monkey, we predefined time intervals of interest for both microsaccadic inhibition (e.g., 70–180 ms after stimulus onset in all monkeys) and postinhibition (e.g., 180–340 ms after stimulus onset) periods. For each experimental condition, we computed the mean microsaccade rate within such a predefined interval and found its extreme value (i.e., the minimum mean inhibition rate or the maximum mean rebound rate) and its latency relative to stimulus onset. Then, we calculated the difference in these values between two given conditions. To obtain the null experimental distribution, we did the same procedure as described earlier in this section: we collected the trials from both conditions into a single data set and randomly permuted their labels, while keeping the initial ratio of the numbers of trials across conditions. We repeated this procedure 1,000 times and, on each iteration, we recalculated the test statistics (i.e., the differences between the rate values and their latencies, when applicable). Finally, we computed the Monte Carlo *P* values of the observed experimental differences by assessing the probability of getting the null-hypothesis test values at least as extreme as the observed experimental values. Significance was classified based on a critical α level of 0.05. This procedure also helped us to ensure that we did not miss any effect with the cluster-based permutation analyses due to different temporal dynamics of the inhibition and postinhibition phases of the microsaccadic rate signature across conditions.

To assess the effect of stimulus polarity on microsaccade directionality irrespective of the microsaccade rate, we compared the fractions of congruent microsaccades (i.e., the sum of microsaccades toward the flash divided by the sum of all microsaccades that occurred in a given time bin) over time between the black and white localized flashes. For this purpose, we used a bootstrapping procedure to obtain the estimates of their dispersion. In particular, we randomly resampled our data with replacement 1,000 times and computed the fraction of congruent microsaccades for each sample. The central tendency measure and the estimate of its standard error were retrieved by calculating the mean and standard deviation of the bootstrap distribution.

Finally, when comparing fractions of congruent microsaccades across conditions, we complemented the data visualization in the figures with microsaccade frequency histograms as a function of time, with bin widths of 24 ms and normalized with respect to the total number of trials in a given condition. This was done to provide an easier visual comparison between direction effects and microsaccade rate. Such histograms are shown at the bottom of each panel in the corresponding figures; their scales are arbitrary with respect to the *y*-axis but kept proportional across conditions within a given monkey.

Note that in all figures, we displayed individual monkey results separately. However, we also always added panels showing grand average data from all trials of all monkeys combined together. This allowed us to visualize which effects were most consistent across all three monkeys, and it was also justified by the overall approximate similarity of trial numbers across the animals. However, as just stated, all statistical tests were always performed only on a per-monkey basis.

Data Availability

All saccade data arrays presented in this paper are available on https://osf.io/psd8t/files/.

RESULTS

We documented the properties of the microsaccadic rate signature in three rhesus macaque monkeys as a function of either visual stimulus size—diffuse (full-screen flash condition) versus localized (localized flash condition)—or visual stimulus polarity—white versus black. Our full-screen flash condition created a diffuse stimulus over an extended range of the visual environment (approximately ±15° horizontally and ±11° vertically for monkeys M and A; and approximately ±22° horizontally and ±13° vertically for monkey F). On the other hand, our localized flash was much smaller ($1 \times 1°$ centered at 2.1° eccentricity). Both kinds of flashes were presented for only one display frame (~8 ms for monkeys M and A and ~7 ms for monkey F) over a uniform gray background filling the display (METHODS), and they were both completely irrelevant to behavior (the task was just to maintain fixation); the rest of the laboratory was dark.

Microsaccadic Inhibition is Largely Similar for Diffuse and Localized Visual Flashes, but Microsaccadic Rebound is Significantly Weaker for Diffuse Flashes

Figure 1 shows example raw rasters of microsaccade onset times across trials from one monkey (M) when a white flash was presented. In the figure, trials from either localized (Fig. 1, *A* and *B*) or diffuse (Fig. 1*C*) flashes were grouped together for easier visibility, but they were randomly interleaved in the experiments. Control trials without any flashes were also collected (Fig. 1*D*). The overlaid continuous curves show our conversion of the discrete microsaccade onset times into microsaccade rate estimates for the different conditions (METHODS). As can be seen, both localized and diffuse flashes caused robust inhibition of microsaccades with a short latency. After the inhibition, microsaccades started to occur again ~140–160 ms after flash onset, but there were differences as a function of flash size. We summarize characteristics inferred from these raw observations in the text and analyses that follow, and across all conditions and all monkeys.

We first asked whether microsaccadic inhibition would systematically occur for both localized and diffuse flashes, and whether it would exhibit different properties across them. For example, if microsaccadic inhibition is a function of sensory neuron properties (as alluded to in INTRODUCTION), then could surround suppression effects (51, 52) associated with large, diffuse stimuli weaken or delay the occurrence of microsaccadic inhibition? If so, then this would implicate specific sensory areas, which are particularly sensitive to

surround suppression effects, in contributing to the inhibition phase of the microsaccadic rate signature.

We plotted microsaccade rate as a function of time from stimulus onset for either diffuse or localized flashes (METHODS). Figure 2*A* shows results with a localized white flash in monkey M, and Fig. 2*B* shows results with a diffuse (full-screen) white flash in the same monkey. In each panel, the gray curve shows microsaccade rate in the control condition in which no stimulus flash was presented (the two gray curves in the two panels are therefore identical). The red and blue horizontal bars on the *x*-axis of each plot show the significant clusters of time in which microsaccade rate was higher (red) or lower (blue) than in control (cluster-based permutation tests; METHODS). The results for the second monkey, A, are shown in Fig. 2, *D* and *E*, and those for the third monkey, F, are shown in Fig. 2, *G* and *H*. Grand averages across all monkeys are shown in Fig. 2, *J* and *K* (METHODS).

In all monkeys, early microsaccadic inhibition occurred equally robustly regardless of whether the stimulus was diffuse or localized. That is, shortly after stimulus onset, there was a robust decrease in microsaccade likelihood before a subsequent rebound (compare colored to gray curves). The similarity of such decrease between the two stimulus types (localized versus diffuse) can be better appreciated by inspecting Fig. 2, *C*, *F*, *I*, and *L*, in which we plotted the microsaccade rate curves for the diffuse and localized flashes

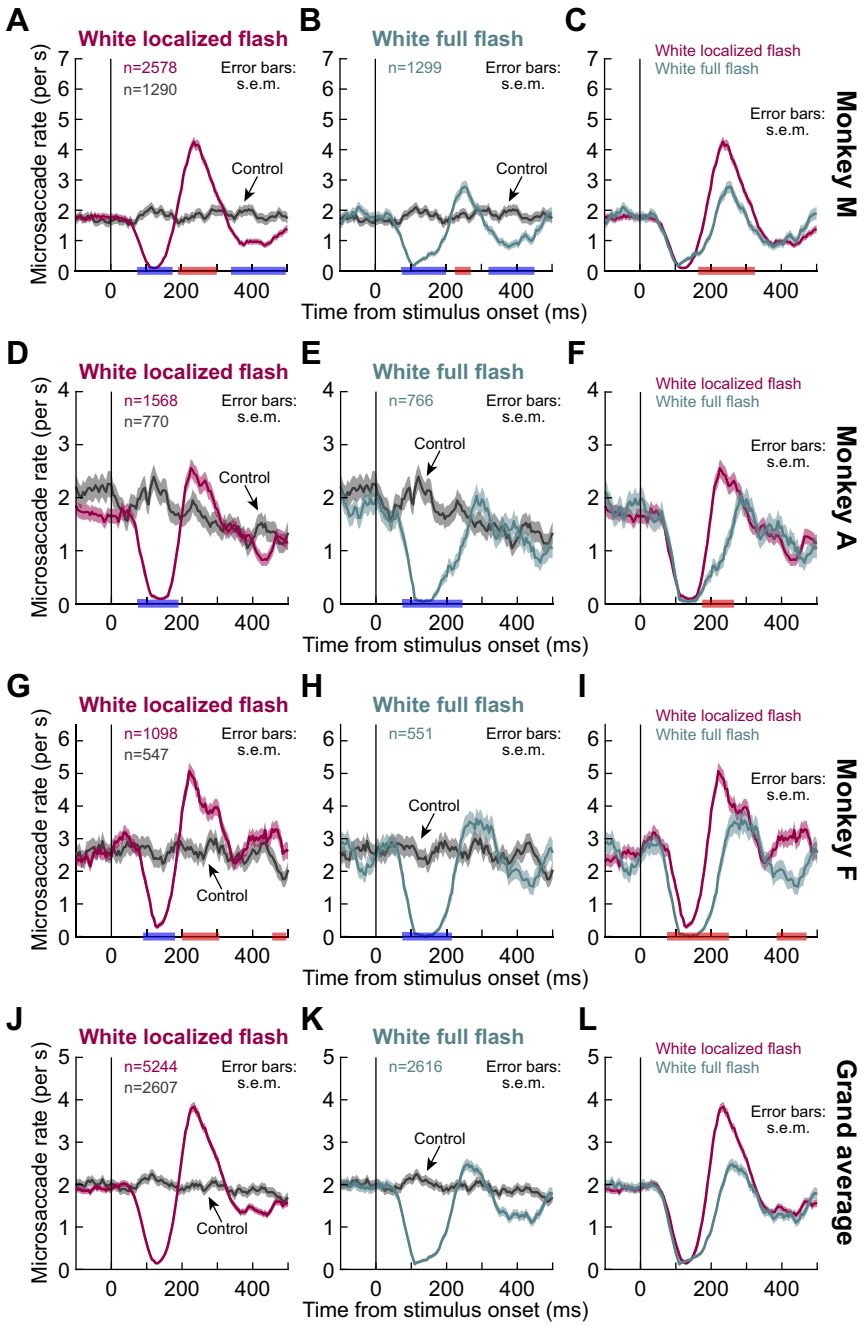

Figure 2. Microsaccade rate signatures with localized and diffuse visual stimuli. *A*: microsaccade rate in monkey M when a white localized flash appeared to the right or left of central fixation. The gray curve shows control microsaccade rate from trials in which the flash was absent. Relative to baseline control rates, microsaccade rate after flash onset decreased rapidly before rebounding. The rebound rate was higher than the control rate. At even longer intervals, microsaccade rate decreased again. Error bars denote SE bounds around each curve (METHODS). The red and blue labels on the *x*-axis indicate positive (red) and negative (blue) significant clusters for the difference between conditions (flash minus control) (METHODS). *B*: same data but when a full-screen flash was used. The early inhibition was similar to *A*, but the rebound was weaker. *C*: microsaccadic rate signatures from *A* and *B* plotted together for easier comparison. Significance clusters on the *x*-axis now indicate whether the localized flash curve was higher (red) or lower (blue) than the full-screen flash curve. Significance in this case (i.e. the time points indicated on the *x*-axis) indicates that the two curves were different in absolute value regardless of the sign of the difference (METHODS). *D*–*F*: same as *A*–*C*, but with monkey A data. Similar conclusions could be reached. *G*–*I*: same as *A*–*C* but for monkey F data. *J*–*L*: same as *A*–*C* but for the grand average data combining trials from all three monkeys together (note that in this and all other figures, we do not show statistics for grand average data, since statistics were performed on a per-monkey basis; METHODS). Microsaccadic inhibition was similar for localized and diffuse flashes, but microsaccadic rebound was different.

together. As can be seen, only monkey F consistently showed earlier and stronger microsaccadic inhibition for the diffuse flashes relative to the localized flashes, which could be due to the larger display size used for this particular monkey (METHODS). In the other two monkeys, and in the grand average, microsaccadic inhibition was highly similar for the diffuse and localized flashes.

Statistically, decreases in microsaccade rate started as early as 75–90 ms after stimulus onset in the localized white-flash condition in all monkeys. For monkeys M and A, inhibition (relative to control) started at 75 ms, and for monkey F, the value was 90 ms ($P = 0$ for all monkeys). With the diffuse flashes, inhibition started at 75 ms for all monkeys ($P = 0$ for all monkeys). These values were assessed using cluster-based permutation tests comparing the control condition to either the localized or diffuse flash conditions (METHODS). We also used similar cluster-based permutation tests to investigate the difference in timing between inhibition onset for the localized and diffuse flashes (METHODS). As stated above, in monkey F, there was a difference in rate starting at 75 ms ($P = 0$), suggesting that inhibition in this monkey started earlier for diffuse than localized flashes (Fig. 2*I*). This was not the case in the other two monkeys (Fig. 2, *C* and *F*), for which a smaller and slightly dimmer display was used.

Similar observations could also be made for black localized and diffuse flashes. For monkey F, there was still a rate difference between the localized and diffuse conditions starting at 70 ms after stimulus onset ($P = 0$), consistent with a slightly later inhibition for the localized flashes (exactly like this monkey showed with white stimuli in Fig. 2*I*). In all monkeys, the time to peak inhibition was also highly similar between localized and diffuse flashes, whether they were white or black; the only statistically significant effect was a 10 ms difference in the time of peak inhibition in monkey F with white flashes (localized earlier than diffuse; $P = 0.038$).

In terms of the strength of microsaccadic inhibition, we measured microsaccade rate at the minimum after stimulus onset in the different conditions. As stated above, and as can also be seen from Fig. 2, only monkey F showed a stronger inhibition for diffuse versus localized flash conditions, both for white ($P = 0.001$) and black ($P = 0.041$) conditions. Again, this might reflect the larger and higher dynamic range in the display device that was used for this monkey (METHODS). A small opposite effect was observed in monkey M but only with black flashes ($P = 0.022$).

Therefore, to summarize the results so far, microsaccadic inhibition was largely similar with diffuse and localized visual stimuli. This adds to our earlier observations that even a simple luminance transient on the fixation spot itself is sufficient to induce strong microsaccadic inhibition (3).

After the microsaccadic inhibition phase, there was a very clear difference in the rebound phase of the microsaccadic rate signature between the localized and diffuse flashes. In Fig. 2, *B, E, H,* and *K*, it can be seen that with full-screen flashes, postinhibition microsaccade rate largely just returned to the baseline control rate without as clear a "rebound" as in the case of the localized flashes (also seen clearly in Fig. 2, *C, F, I,* and *L*). Targeted permutation tests revealed no difference in peak microsaccade rate (relative to control) in a predefined rebound interval (METHODS) in monkeys A and F ($P = 0.256$ and 0.101, respectively), and there was a moderate rebound effect in monkey M (peak rate difference = 0.719 microsaccades/s, $P = 0$; permutation test). This is quite different from how microsaccade rate rebounded in a stronger fashion after the inhibition that was caused by localized flashes (Fig. 2, *A, D, G,* and *J*); peak rate was almost two times the baseline control rate in monkeys M and F (peak rate difference = 2.196 and 2.069 microsaccades/s for M and F, respectively, $P = 0$; permutation test) and ~1.3 times the baseline control rate in monkey A (mean peak rate difference = 0.609 microsaccades/s, $P = 0.033$; permutation test).

We also statistically compared the rate curves obtained with diffuse and localized flashes with each other by plotting them together (Fig. 2, *C, F,* and *I*). Cluster-based permutation tests revealed a significant difference between conditions in the rebound phase for all monkeys (starting at 165 ms and 175 ms after stimulus onset for monkeys M and A, respectively; $P = 0$; for monkey F, we did not search for a time since rate was different also early on during inhibition, as seen in Fig. 2*I*). As can be seen from Fig. 2, *C, F, I,* and *L*, peak microsaccade rate after the inhibition phase with localized flashes was more than 1.3 times stronger than peak microsaccade rate after the inhibition phase with diffuse flashes in all monkeys. We quantified these effects by running permutation tests on the peak rate values and their latencies. In monkey M, the mean peak rate difference between localized and diffuse flashes was 1.478 microsaccades/s ($P = 0$), and the latency difference was −20 ms ($P = 0.005$). These values were 0.522 microsaccades/s ($P = 0.034$) and −60 ms ($P = 0.001$), respectively, for monkey A. For monkey F, the peak rate difference was 1.464 microsaccades/s ($P = 0$), but the latency difference was not significant ($P = 0.062$).

With black flashes, similar conclusions could also be reached concerning the postinhibition rebound phase with diffuse versus localized flashes. In this case, significant differences between diffuse and localized conditions in the postinhibition period emerged 165 ms after stimulus onset for both monkeys M and A (as with white flashes, the statistical start of the rebound phase could not be determined in monkey F due to significantly weaker inhibition caused by localized flashes). Moreover, once again, with localized flashes, microsaccade rate reached its peak earlier in monkeys M and F (latency difference = −45 ms, $P = 0$ for monkey M and latency difference = −25 ms, $P = 0.017$ for monkey F; permutation tests) and rose higher in monkeys M and A (mean peak rate difference = 2.696 microsaccades/s, $P = 0$ for monkey M and mean peak rate difference = 1.838 microsaccades/s, $P = 0$ for monkey A; permutation tests) than with diffuse stimuli; similar trends in the mean peak rate for monkey F ($P = 0.41$) and the mean peak latency for monkey A ($P = 0.143$) existed.

To further clarify whether the weaker postinhibition microsaccadic rebound with diffuse flashes depended on stimulus polarity, we next plotted the white and black diffuse flash curves together (Fig. 3). In the rebound phase, each monkey showed different effects from the others. Monkey F showed a stronger rebound for black diffuse flashes ($P = 0$; cluster-based permutation test), whereas monkey A showed the opposite effect ($P = 0.014$). Monkey M, in turn, showed no difference between white and black diffuse flashes. All statistical comparisons are highlighted in Fig. 3.

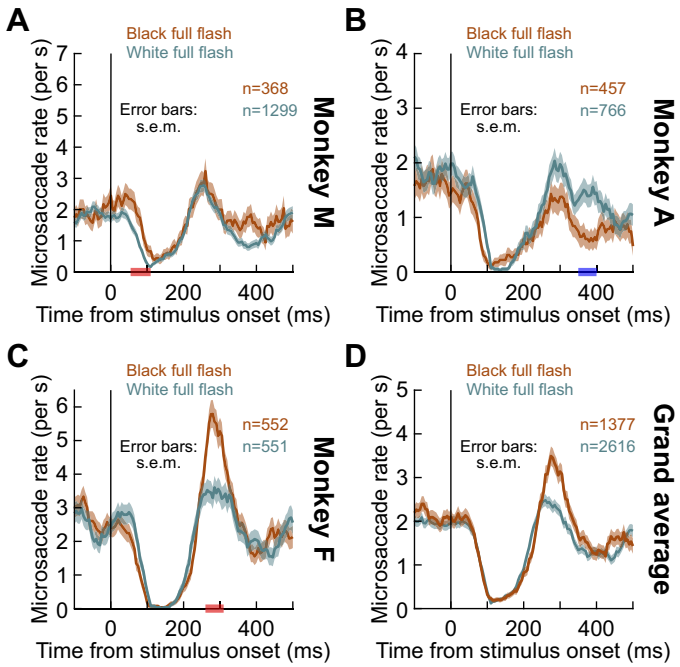

Figure 3. Microsaccade rate signatures with black and white diffuse visual stimuli. For each monkey, we plotted microsaccade rates from Fig. 2, this time directly comparing black vs. white full-screen flashes. In all but monkey M (red horizontal bar in *A*), there were no significant differences between black and white diffuse flashes in terms of initial microsaccadic inhibition. For subsequent microsaccadic rebound phases, the monkeys differed in their effects. Colored intervals on the *x*-axes delineate significant intervals of negative or positive mean differences between microsaccade rates in the black and white conditions (obtained with one-sided cluster-based permutation tests). All other conventions are similar to Fig. 2. In *D*, we show the grand average data after pooling all monkeys together (METHODS). Microsaccadic inhibition was highly similar between black and white diffuse flashes, but the rebound showed differential effects based on the idiosyncratic effects in *A*–*C*.

Therefore, the above results, so far, suggest that diffuse visual stimuli are as effective as localized visual stimuli in causing robust microsaccadic inhibition in rhesus macaque monkeys (Figs. 1 and 2). However, postinhibition microsaccade rates can be lower with diffuse stimuli (Fig. 2). Moreover, these effects with diffuse stimuli are largely independent of stimulus polarity (Fig. 3), with particularly idiosyncratic differences between the different monkeys in the postinhibition rebound phase of the microsaccadic rate signature. This suggests that this rebound phase may be neurophysiologically distinct from the early inhibition phase, consistent with (7); see DISCUSSION.

Black Localized Flashes have Stronger "Cueing Effects" than White Localized Flashes

With localized flashes, we saw in Fig. 2 that the microsaccadic rate signature looked more similar to classic literature descriptions. That is, there was a strong postinhibition rebound in microsaccade rate, reaching levels significantly higher than baseline microsaccade-rate during steady-state fixation. We next wondered whether this was additionally influenced by stimulus polarity. Unlike in Fig. 3 for the case of diffuse flashes, there was indeed a consistent effect of black localized flashes on the microsaccadic rate signature across all three monkeys. This effect can be seen in Fig. 4; black localized flashes were particularly effective in modulating the postinhibition rebound phase of the microsaccadic rate signature, as was also confirmed by cluster-based permutation tests (the red horizontal bars on the *x*-axes in Fig. 4 indicating the regions of significantly stronger rebound immediately after the inhibition with black flashes; $P < 0.015$ for all monkeys). These postinhibition rebound observations cannot be explained by stimulus contrast alone, because the contrast of the black flash relative to the background luminance was lower than the contrast of the white flash relative to the background luminance (METHODS). In terms of the initial microsaccadic inhibition phase, neither cluster-based permutation tests nor targeted permutation tests revealed significant differences in microsaccade rate in all three monkeys. Thus, with localized flashes, stimulus polarity had the largest effect on the rebound phase of the overall microsaccadic rate signature.

That said, because localized visual stimuli have a directional component associated with them, they resemble "cues" in classic attentional cueing tasks. Past work has shown how such cues, even when behaviorally irrelevant (3, 5), are associated with very systematic directional

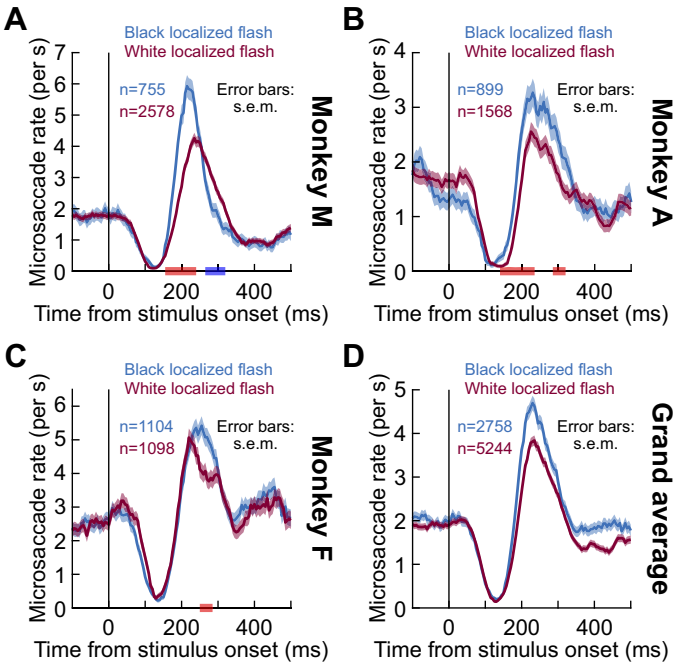

Figure 4. Microsaccade rate signatures with black and white localized visual stimuli. For each monkey, we plotted microsaccade rates comparing black vs. white localized flashes, and we performed their time-course analyses with the cluster-based permutation tests described in METHODS. The red and blue labels on the *x*-axes indicate significant intervals of positive and negative mean differences, respectively, between microsaccade rates in the black and white localized flash conditions, obtained with a critical α level of 0.05 (i.e., one-sided tests; METHODS). In all monkeys, the immediate postinhibition microsaccadic rebound stage of the rate signature was significantly stronger with black than white localized flashes (first red horizontal bar after each inhibition phase). This is different from the effects of stimulus polarity that we saw with diffuse flashes (Fig. 3). All other conventions are similar to Fig. 2. In *D*, we show the grand average results after pooling data from all monkeys together (METHODS). Microsaccadic inhibition was similar for black vs. white localized flashes. However, microsaccadic rebound was consistently stronger for black flashes (*A*–*C*).

modulations of microsaccades when they appear under steady-state fixation conditions. When viewed from the perspective of the microsaccadic rate signature, these direction modulations consist of two primary effects: *1*) a later inhibition of microsaccades that are congruent (in their direction) with stimulus location when compared with the inhibition time of microsaccades that are incongruent with stimulus location; and *2*) a stronger and earlier postinhibition rebound for microsaccades that are incongruent with stimulus location than for congruent microsaccades (1, 5, 6, 9, 24). In other words, microsaccades that do occur early after stimulus onset tend to be strongly biased towards the stimulus location, and microsaccades occurring late after stimulus onset tend to be biased in the opposite direction, and this is believed to reflect an interaction between ongoing microsaccade motor commands and visual bursts associated with stimulus onsets (3, 5). When we analyzed microsaccadic rate signatures for different microsaccade directions in our localized flash conditions, we confirmed these expected results; most interestingly, black stimuli amplified the timing differences in early microsaccadic inhibition between congruent and incongruent movements, whereas the stimulus polarity effects on postinhibition microsaccadic rebound effects (when separated by movement direction) were more variable.

Specifically, in Fig. 5, we plotted the rate of congruent and incongruent microsaccades separately. Congruent microsaccades were defined as those with directions towards the stimulus hemifield, and incongruent ones were defined as those opposite the stimulus hemifield (METHODS). As can be seen, congruent microsaccades were indeed harder to inhibit than incongruent microsaccades in all three monkeys, suggesting that in these early times after stimulus onset, if a microsaccade were to occur, it was more likely to be directed towards the flash location (3, 5, 9, 24). We confirmed that this early inhibition effect was consistent in all three monkeys by performing targeted permutation tests on the time to peak inhibition (METHODS): all three monkeys showed statistically significant earlier inhibition of incongruent microsaccades than congruent microsaccades, and this was also true for either black or white flashes ($P < 0.031$ across all relevant comparisons between congruent and incongruent microsaccadic inhibition onsets in each individual monkey and each individual stimulus polarity). This observation is evident in Fig. 5 as an earlier reduction in microsaccade rate for all incongruent curves when compared with all corresponding congruent rate curves. Note that the figure also shows the results of the cluster-based measurements on the *x*-axes, for consistency with all other figures, but the timing of inhibition as a function of microsaccade direction is what is relevant here. Interestingly, this early "cueing" effect in the microsaccadic rate signature (i.e., during the early inhibition phase) was clearly stronger with black than white stimuli. This can be seen by the larger

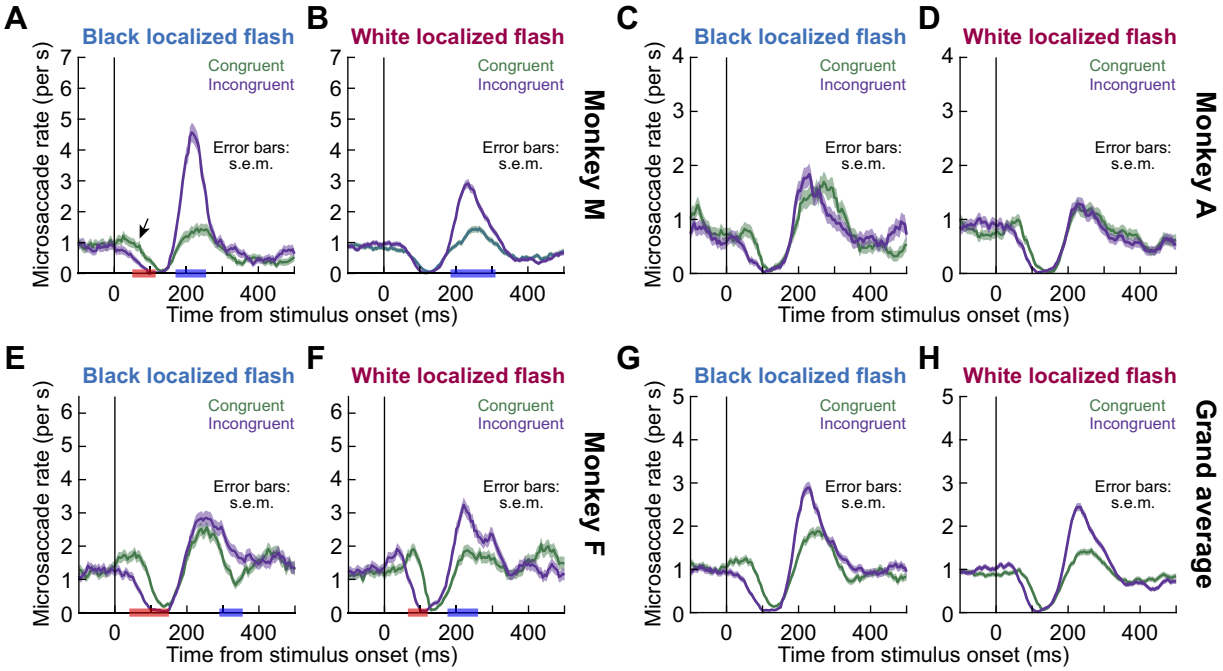

Figure 5. Microsaccade rate signatures with black and white localized visual stimuli when separated based on microsaccade direction. *A*: microsaccade rate in monkey M computed separately for congruent and incongruent microsaccades. Congruent microsaccades were defined as those movements directed toward the flash location, and incongruent microsaccades were defined as the microsaccades directed opposite the flash location (METHODS). This panel shows results with a black flash. Consistent with earlier results, congruent microsaccades were harder to inhibit than incongruent microsaccades (earlier inhibition onset for incongruent microsaccades; black arrow). *B*: with white localized flashes, the difference between the congruent and incongruent curves was smaller overall than in *A*, particularly in the early inhibition phase. *C* and *D*: similar analyses to *A* and *B* for monkey A. Early directional differences associated with microsaccadic inhibition were weaker with white flashes (*D*) but amplified with black flashes (*C*). Rebound effects were weaker than in monkey M. *E* and *F*: in monkey F, the early inhibition effects, and their dependence on stimulus polarity, were similar to monkey M. Postinhibition rebounds were once again variable in relation to the other two animals. All other conventions are similar to Fig. 2. Red and blue bars on *x*-axes show significant clusters of positive (red) and negative (blue) mean differences at the critical α level of 0.05 (METHODS). *G* and *H*: results from the grand average population pooling data from all three monkeys together (METHODS). The difference between congruent and incongruent curves in the early inhibition phase was magnified with black flashes when compared with white ones.

difference between congruent and incongruent curves in all three monkeys for black stimuli when compared with white ones (in the early inhibition phase; also see Fig. 6 below). Therefore, even though the overall microsaccadic rate signature did not reveal strong differences in the initial microsaccadic inhibition phase between black and white flashes (Fig. 4), separating microsaccades by their congruency with stimulus location did reveal stronger early "cueing effects" on the movements with black stimuli.

In the postinhibition phase, the impact of stimulus polarity was, on the other hand, variable across the monkeys. Monkey M showed stronger incongruent microsaccade rebound for black flashes (Fig. 5, *A* and *B*), but monkey F showed stronger incongruent microsaccade rebound for white flashes (Fig. 5, *E* and *F*). Monkey A showed nonsignificant trends consistent with monkey M (Fig. 5, *C* and *D*). Therefore, once again, the postinhibition microsaccadic rebound phase was the most variable among the monkeys in terms of stimulus polarity and its relation to the directional rate curves.

To summarize, black localized flashes were associated with stronger microsaccadic rate modulations in all three monkeys (Fig. 4), and there was also a directional component associated with the dependence of the earliest poststimulus microsaccades (during the early inhibition phase) on stimulus polarity (Fig. 5). So-called early cueing effects on microsaccades were, thus, stronger with black than white localized flashes, particularly in the initial microsaccadic inhibition phase.

To further investigate this idea of stronger directional effects with black stimuli in the early inhibition phase, we next assessed microsaccade directions independently of microsaccade rates. For each time bin relative to localized flash onset time, we computed the fraction of microsaccades that both occurred within this time bin and were also congruent with flash location. This gave us a time course of microsaccade directions relative to the flash location. We did this separately for black and white flashes. These results are shown in Fig. 6, in which we also superimposed histograms of all microsaccade times in each flash condition to visually relate the microsaccade direction time courses with the microsaccadic rate signatures (the histograms in Fig. 6 are essentially another way to visualize the same rate curves of localized flashes in Figs. 1 and 2). As can be seen, in all three monkeys, the likelihood of getting a microsaccade directed toward the flash sharply increased after stimulus onset, peaking at the time of maximal inhibition, which is consistent with previous findings (3, 5, 9, 24, 53). In the postinhibition period, this pattern started to reverse, again consistent with prior results (3, 5, 9, 24), although the known postinhibition direction reversals were more variable across monkeys in the current task of behaviorally irrelevant flashes (for example, monkey A barely showed a bias for oppositely directed microsaccades after the end of microsaccadic inhibition). Nonetheless, all three monkeys showed an earlier and longer lasting biasing of early microsaccades (during the microsaccadic inhibition phase) toward the flash location with black stimuli when compared with white ones, consistent with Fig. 5.

In monkey M, the black flashes were also associated with more opposite microsaccades in the rate rebound phase after microsaccadic inhibition when compared with the white flashes, but this was the opposite in the case of monkey F (and monkey A for a brief moment). This again demonstrates that postinhibition microsaccades were most susceptible to interindividual differences in our task, in which the stimulus onsets were completely irrelevant to successful task performance.

DISCUSSION

We investigated the effects of stimulus polarity and size on the microsaccadic rate signature after stimulus onsets.

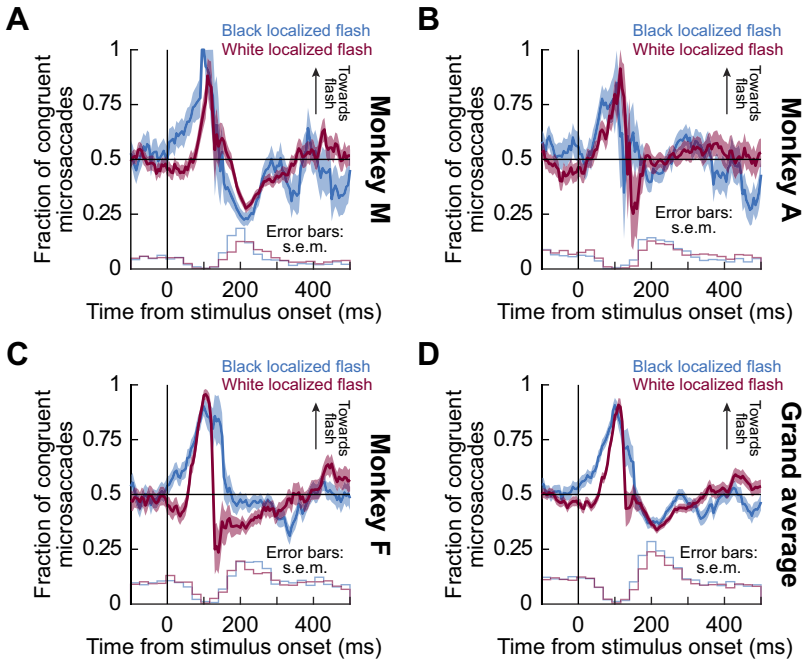

Figure 6. Distribution of microsaccade directions relative to localized flash location for black and white flashes. The thick curves with error bars show the time courses of fractions of microsaccades directed toward the flash location under either white or black localized flash conditions. The means and their standard errors were computed using bootstrapping with replacement. The histograms at the bottom of each panel show in the corresponding color the frequency of all microsaccades, regardless of their direction, that happened under the black and white localized flash conditions. The histograms were normalized with respect to the number of trials in a given condition; their scales are arbitrary with respect to the *y*-axis but kept proportional to each other within a given monkey. In all monkeys, the fraction of congruent microsaccades increased during the inhibition phase and started to decrease at the beginning of the rebound period. In addition, all monkeys showed an earlier and more sustained inhibition of incongruent microsaccades with black stimuli (i.e. stronger directional modulation toward the flash location). All other conventions are similar to Fig. 2. In *D*, we show the grand average results when pooling across monkeys. A clearly stronger cueing effect on microsaccade directions with black localized flashes, when compared with white ones, can be seen during the early inhibition phase of the microsaccadic rate signature.

We exploited the fact that even subtle and highly fleeting flashes of only ~7–8 ms duration are sufficient to cause rapid microsaccadic inhibition after their occurrence followed by a rebound in microsaccade rate. We found that the inhibition was similar for small, localized flashes and large, diffuse ones. However, the subsequent rebound was largely absent and delayed with the latter flashes. In terms of stimulus polarity, we saw the most systematic differences between white and black flashes in the localized flash conditions. For these localized flash trials, black stimuli caused more substantial changes in the microsaccadic rate signature overall than white ones.

Our results can inform hypotheses about the neural mechanisms for microsaccadic and saccadic inhibition. In Hafed and Ignashchenkova (5), we hypothesized that the rate signature reflects visual neural activity in oculomotor areas such as, but not exclusively restricted to, the SC. We specifically hypothesized that the dissociation between rate and direction effects (also present in our own data; e.g., Fig. 6) might reflect spatial readout of SC visual activity for the direction effects (3) but additional, and potentially different, use of visual activity by the oculomotor system to inhibit saccades for the rate effects (5). Consistent with this, in our current experiments, the similarity that we observed for microsaccadic inhibition between small and large stimuli (Figs. 1 and 2) suggests that the early rate effect (i.e., microsaccadic inhibition) is an outcome of early sensory activity that is not necessarily strictly spatial in organization. We hypothesized earlier (5) that a candidate area for realizing such rapid saccadic inhibition could be a late motor area with access to early sensory information. Our ongoing experiments (54), comparing V1, SC, and brainstem omnipause neurons (55–57), support the hypothesis that it is visual sensory responses by omnipause neurons that are most likely to mediate saccadic inhibition. This would be consistent with our present observations on similar inhibition between small and large stimuli.

The difference in postinhibition microsaccadic rebound that we observed between small and large stimuli is also consistent with spatially organized maps for the spatial components of saccadic inhibition (3, 5). Specifically, with localized flashes, spatial readout of visual stimulus location, say in SC, would cause direction oscillations of microsaccades (24). On the other hand, diffuse stimuli centered on fixation would activate symmetric populations of neurons simultaneously. This might not "attract" early microsaccades in any one direction and therefore alleviates the need for opposite microsaccades to occur later in the postinhibition microsaccadic rebound phase. Thus, with diffuse and symmetric flashes, early microsaccades near the inhibition phase would not introduce large foveal eye position errors like might happen with small, localized peripheral cues. As a result, there would be no need to trigger corrective microsaccades after the inhibition. Indeed, in our earlier work, we showed that shaping the landscape of peripheral visual activity in an oculomotor map, either with extended bars or with simultaneous stimulus onsets at multiple locations, not only influences the directions of early microsaccades, but also affects subsequent postinhibition microsaccades, which become oppositely directed from the earlier ones (5). Moreover, we later confirmed that eye position error was indeed an important factor in whether microsaccades were triggered or not (9, 24). Naturally, in behaviors such as reading, in which the subsequent forward saccade after any flash is a necessity imposed by the behavioral task at hand, full-screen flashes would be expected to exhibit some postinhibition rate rebound. This was shown previously (19), although even in that study, rebound rates were higher with localized flashes.

The aforementioned interpretations are also highly consistent with mathematical models of fixational eye movements that were recently proposed by Engbert et al. (28, 29) and motivated by earlier studies of the dynamics of microsaccade rate and direction in a variety of attentional tasks (4, 6, 27). Specifically, these models focused on two-dimensional dynamics of fixational eye movements, including both intermicrosaccadic ocular position drifts as well as microsaccades themselves. According to these models, a self-avoiding random walk process, governed by an oculomotor potential, results in spatial and temporal dynamics of drift displacements that are consistent with experimental observations (29). On top of these displacements, microsaccades are triggered when the eye deviates beyond a threshold in the oculomotor potential. Interestingly, to model the impacts of sensory and attentional modulations on the microsaccadic rate signature, Engbert et al. (28) also invoked a role for early sensory signals to mediate microsaccadic inhibition, and, in addition, a combination of delayed sensory signals and attentional signals to mediate subsequent microsaccadic rebound. These ideas are consistent with the hypothesis that microsaccadic rebound is dissociable from early microsaccadic inhibition (7).

Indeed, it is intriguing that the largest effects of stimulus polarity on overall microsaccade rate in our experiments appeared on the postinhibition rebound phase after small, localized flashes (Fig. 4). In our earlier models, we had modeled postinhibition microsaccades as being driven with greater "urgency" than baseline microsaccades (5, 24) as if there is extra drive associated with them, needed to recover from the disruptions caused by the stimulus onsets. Similarly, in the Engbert models (28), oculomotor potential thresholds were reduced, by a combination of sensory and attentional signals, specifically for the rebound microsaccades. As mentioned in the Introduction, when we reversibly inactivated FEF, we found that the greatest effects on the microsaccadic rate signature were on postinhibition microsaccades (7), suggesting that the extra drive might come from frontal cortical areas. This might make sense in retrospect: although inhibition may be mediated by rapid, reflexive responses of the oculomotor system to sensory stimulation, postinhibition eye movements might reflect processes attempting to recover from external disruptions to the ongoing oculomotor rhythm. These processes likely involve additional drive from cortex, a suggestion also made for large saccades (58). Our current results of differential effects of black localized stimuli on postinhibition microsaccades add to the evidence that different components of the microsaccadic rate signature (e.g., inhibition vs. rebound) are governed by distinct and dissociable neural mechanisms.

From this perspective, it is worth observing that the largest differences among the individual monkeys repeatedly occurred in the rebound phase of the microsaccadic rate signature. Specifically, throughout our results, we highlighted

cases in which the different individuals differed in their effects. For example, monkey A did not show as clear a late directional rebound effect like the other two monkeys when we separated congruent and incongruent microsaccade directions (Figs. 5 and 6). Similarly, monkey F had opposite stimulus polarity effects in the rebound microsaccade directions when compared with monkey M (Fig. 6). Finally, the three monkeys had either stronger or weaker or similar post-microsaccadic rebound rate for black diffuse stimuli when compared with white ones (Fig. 3). These individual differences were likely attributed in our case to the fact that the flashes were completely behaviorally irrelevant. That is, if postinhibition microsaccades are driven by top-down cortical factors (7), then it may be expected that the lack of behavioral relevance for the flashes in our experiments would be associated with the largest interindividual differences. Interestingly, despite such interindividual differences, we think that simple parameter changes of existing models can account for such differences. For example, using our earlier models of the microsaccadic rate signature (5, 24), we could show in Tian et al. (24) how a single model, and only simple parameter changes, could account for often-large individual differences among 22 different subjects performing a standard cueing task.

Concerning why or how stimulus polarity revealed the differences described in this study, we think that lags between black and white flashes during inhibition (e.g., Figs. 5 and 6) might reflect the differences in time that it takes to propagate visual information from the retina to other structures for dark versus light stimuli. For example, it was shown that darks propagate faster than lights to visual cortex due to functional asymmetries in ON and OFF visual pathways (e.g., in humans: 59; in cats: 45, 60, 61). It is interesting that such asymmetry might differentially affect congruent and incongruent microsaccades in the very early microsaccadic inhibition phase, as we saw in Figs. 5 and 6 for all monkeys. It is also interesting that for larger saccades during reading (21), black flashes also seemed to cause stronger inhibition, but the problem there was that their white flashes did not occlude the black text; thus, their white flashes were likely lower in contrast than their black flashes.

Regardless of the exact causes, our results on stimulus polarity might also be relevant for attention studies (62–64) as microsaccades are often described as a biomarker for attentional shifts (4, 6, 9, 24, 27, 53). For example, there appear to be mixed results for cue luminance manipulations in cueing paradigms. In these manipulations, varying the cue luminance energy is usually coupled with varying stimulus contrast relative to the background (e.g., 33, 65–67). Thus, dark cues are necessarily perceptually degraded when compared with bright cues, because of their reduced contrast. Our results suggest that investigations of early facilitation and subsequent inhibition of return effects in attentional cueing paradigms can reveal interesting findings when taking stimulus polarity into account.

GRANTS

This study was funded by the Deutsche Forschungsgemeinschaft (DFG) through the Research Unit: FOR 1847 (Project: HA6749/2-1). The study also funded by the Werner Reichardt Centre for Integrative Neuroscience (CIN; DFG EXC307). T.M. and Z.M.H. were additionally supported by a CIN intramural grant (Mini_GK 2017-04).

DISCLOSURES

No conflicts of interest, financial or otherwise, are declared by the authors.

AUTHOR CONTRIBUTIONS

Z.M.H. conceived and designed research; A.B. and Z.M.H. performed experiments; T.M., A.B., and Z.M.H. analyzed data; T.M., A.B., and Z.M.H. interpreted results of experiments; T.M. and Z.M.H. prepared figures; T.M., A.B., and Z.M.H. drafted manuscript; T.M., A.B., and Z.M.H. edited and revised manuscript; T.M., A.B., and Z.M.H. approved final version of manuscript.

ENDNOTE

At the request of the authors, readers are herein alerted to the fact that additional materials related to this manuscript may be found at https://osf.io/psd8t/files/. These materials are not a part of this manuscript, and have not undergone peer review by the American Physiological Society (APS). APS and the journal editors take no responsibility for these materials, for the website address, or for any links to or from it.

REFERENCES

1. **Hafed ZM**, **Chen C-Y**, **Tian X.** Vision, perception, and attention through the lens of microsaccades: mechanisms and implications. *Front Syst Neurosci* 9: 167, 2015. doi:10.3389/fnsys.2015.00167.
2. **Bonneh YS**, **Adini Y**, **Polat U.** Contrast sensitivity revealed by microsaccades. *J Vis* 15: 11, 2015. doi:10.1167/15.9.11.
3. **Buonocore A**, **Chen CY**, **Tian X**, **Idrees S**, **Münch TA**, **Hafed ZM.** Alteration of the microsaccadic velocity-amplitude main sequence relationship after visual transients: implications for models of saccade control. *J Neurophysiol* 117: 1894–1910, 2017. doi:10.1152/jn.00811.2016.
4. **Engbert R**, **Kliegl R.** Microsaccades uncover the orientation of covert attention. *Vision Res* 43: 1035–1045, 2003. doi:10.1016/S0042-6989(03)00084-1.
5. **Hafed ZM**, **Ignashchenkova A.** On the dissociation between microsaccade rate and direction after peripheral cues: microsaccadic inhibition revisited. *J Neurosci* 33: 16220–16235, 2013. doi:10.1523/JNEUROSCI.2240-13.2013.
6. **Laubrock J**, **Engbert R**, **Kliegl R.** Microsaccade dynamics during covert attention. *Vision Res* 45: 721–730, 2005. doi:10.1016/j.visres.2004.09.029.
7. **Peel TR**, **Hafed ZM**, **Dash S**, **Lomber SG**, **Corneil BD.** A causal role for the cortical frontal eye fields in microsaccade deployment. *PLoS Biol* 14: e1002531, 2016. doi:10.1371/journal.pbio.1002531.
8. **Rolfs M**, **Kliegl R**, **Engbert R.** Toward a model of microsaccade generation: the case of microsaccadic inhibition. *J Vis* 8: 5.1–5.23, 2008. doi:10.1167/8.11.5.
9. **Tian X**, **Yoshida M**, **Hafed ZM.** Dynamics of fixational eye position and microsaccades during spatial cueing: the case of express microsaccades. *J Neurophysiol* 119: 1962–1980, 2018. doi:10.1152/jn.00752.2017.
10. **Valsecchi M**, **Betta E**, **Turatto M.** Visual oddballs induce prolonged microsaccadic inhibition. *Exp Brain Res* 177: 196–208, 2007. doi:10.1007/s00221-006-0665-6.
11. **White AL**, **Rolfs M.** Oculomotor inhibition covaries with conscious detection. *J Neurophysiol* 116: 1507–1521, 2016 [Erratum in *J Neurophysiol* 118: 648, 2017]. doi:10.1152/jn.00268.2016.
12. **Rolfs M.** Microsaccades: small steps on a long way. *Vision Res* 49: 2415–2441, 2009. doi:10.1016/j.visres.2009.08.010.

13. **Scholes C**, **McGraw PV**, **Nystrom M**, **Roach NW.** Fixational eye movements predict visual sensitivity. *Proc R Soc B* 282: 20151568, 2015. doi:10.1098/rspb.2015.1568.
14. **Bompas A**, **Sumner P.** Saccadic inhibition reveals the timing of automatic and voluntary signals in the human brain. *J Neurosci* 31: 12501–12512, 2011. doi:10.1523/JNEUROSCI.2234-11.2011.
15. **Buonocore A**, **McIntosh RD.** Saccadic inhibition underlies the remote distractor effect. *Exp Brain Res* 191: 117–122, 2008. doi:10.1007/s00221-008-1558-7.
16. **Buonocore A**, **McIntosh RD**, **Melcher D.** Beyond the point of no return: effects of visual distractors on saccade amplitude and velocity. *J Neurophysiol* 115: 752–762, 2016. doi:10.1152/jn.00939.2015.
17. **Edelman JA**, **Xu KZ.** Inhibition of voluntary saccadic eye movement commands by abrupt visual onsets. *J Neurophysiol* 101: 1222–1234, 2009. doi:10.1152/jn.90708.2008.
18. **Reingold EM**, **Stampe DM.** Saccadic inhibition in complex visual tasks. In: *Current Oculomotor Research*, edited by Becker W, Deubel H, Mergner T. Boston, MA: Springer, 1999, p**.** 249–255. doi:10.1007/978-1-4757-3054-8_35.
19. **Reingold EM**, **Stampe DM.** Saccadic inhibition in reading. *J Exp Psychol Hum Percept Perform* 30: 194–211, 2004. doi:10.1037/0096-1523.30.1.194.
20. **Reingold EM**, **Stampe DM.** Saccadic inhibition in voluntary and reflexive saccades. *J Cogn Neurosci* 14: 371–388, 2002. doi:10.1162/089892902317361903.
21. **Reingold EM**, **Stampe DM.** Using the saccadic inhibition paradigm to investigate saccadic control in reading. In: *The Mind's Eye: Cognitive and Applied Aspects of Eye Movement Research*, edited by Hyona J, Radach R, Deubel H. Amsterdam: North Holland, 2003, p**.** 347–360.
22. **Hafed ZM**, **Lovejoy LP**, **Krauzlis RJ.** Modulation of microsaccades in monkey during a covert visual attention task. *J Neurosci* 31: 15219–15230, 2011. doi:10.1523/JNEUROSCI.3106-11.2011.
23. **Hafed ZM**, **Lovejoy LP**, **Krauzlis RJ.** Superior colliculus inactivation alters the relationship between covert visual attention and microsaccades. *Eur J Neurosci* 37: 1169–1181, 2013. doi:10.1111/ejn.12127.
24. **Tian X**, **Yoshida M**, **Hafed ZM.** A microsaccadic account of attentional capture and inhibition of return in posner cueing. *Front Syst Neurosci* 10: 23, 2016. doi:10.3389/fnsys.2016.00023.
25. **Yoshida M**, **Hafed Z.** Microsaccades in blindsight monkeys. *J Vis* 17: 896, 2017. doi:10.1167/17.10.896.
26. **Malevich T**, **Buonocore A**, **Hafed ZM.** Rapid stimulus-driven modulation of slow ocular position drifts. *eLife* 9: e57595, 2020. doi:10.7554/eLife.57595.
27. **Hafed ZM**, **Clark JJ.** Microsaccades as an overt measure of covert attention shifts. *Vision Res* 42: 2533–2545, 2002. doi:10.1016/S0042-6989(02)00263-8.
28. **Engbert R.** Computational modeling of collicular integration of perceptual responses and attention in microsaccades. *J Neurosci* 32: 8035–8039, 2012. doi:10.1523/JNEUROSCI.0808-12.2012.
29. **Engbert R**, **Mergenthaler K**, **Sinn P**, **Pikovsky A.** An integrated model of fixational eye movements and microsaccades. *Proc Natl Acad Sci U S A* 108: 16149–16150, 2011. doi:10.1073/pnas.1102730108.
30. **Chen CY**, **Ignashchenkova A**, **Thier P**, **Hafed ZM.** Neuronal response gain enhancement prior to microsaccades. *Curr Biol* 25: 2065–2074, 2015. doi:10.1016/j.cub.2015.06.022.
31. **Hafed ZM.** Alteration of visual perception prior to microsaccades. *Neuron* 77: 775–786, 2013. doi:10.1016/j.neuron.2012.12.014.
32. **Hawkins HL**, **Shafto MG**, **Richardson K.** Effects of target luminance and cue validity on the latency of visual detection. *Percept Psychophys* 44: 484–492, 1988. doi:10.3758/BF03210434.
33. **Hughes HC.** Effects of flash luminance and positional expectancies on visual response latency. *Percept Psychophys* 36: 177–184, 1984. doi:10.3758/BF03202678.
34. **Kean M**, **Lambert A.** The influence of a salience distinction between bilateral cues on the latency of target-detection saccades. *Br J Psychol* 94: 373–388, 2003. doi:10.1348/000712603767876280.
35. **Reuter-Lorenz PA**, **Jha AP**, **Rosenquist JN.** What is inhibited in inhibition of return? *J Exp Psychol Hum Percept Perform* 22: 367–378, 1996. doi:10.1037/0096-1523.22.2.367.
36. **Buonocore A**, **Skinner J**, **Hafed ZM.** Eye position error influence over "open-loop" smooth pursuit initiation. *J Neurosci* 39: 2709–2721, 2019. doi:10.1523/JNEUROSCI.2178-18.2019.
37. **Skinner J**, **Buonocore A**, **Hafed ZM.** Transfer function of the rhesus macaque oculomotor system for small-amplitude slow motion trajectories. *J Neurophysiol* 121: 513–529, 2019. doi:10.1152/jn.00437.2018.
38. **Brainard DH.** The Psychophysics Toolbox. *Spat Vis* 10: 433–436, 1997.
39. **Kleiner M**, **Brainard D**, **Pelli DG.** What's new in Psychtoolbox-3? (Abstract). *Perception* 36: 1–16, 2007.
40. **Pelli DG.** The VideoToolbox software for visual psychophysics: transforming numbers into movies. *Spat Vis* 10: 437–442, 1997.
41. **Chen C-Y**, **Hafed ZM.** Postmicrosaccadic enhancement of slow eye movements. *J Neuroscience* 33: 5375–5386, 2013. doi:10.1523/JNEUROSCI.3703-12.2013.
42. **Fuchs AF**, **Robinson DA.** A method for measuring horizontal and vertical eye movement chronically in the monkey. *J Appl Physiol* 21: 1068–1070, 1966. doi:10.1152/jappl.1966.21.3.1068.
43. **Judge SJ**, **Richmond BJ**, **Chu FC.** Implantation of magnetic search coils for measurement of eye position: an improved method. *Vision Res* 20: 535–538, 1980. doi:10.1016/0042-6989(80)90128-5.
44. **Komban SJ**, **Alonso JM**, **Zaidi Q.** Darks are processed faster than lights. *J Neurosci* 31: 8654–8658, 2011. doi:10.1523/JNEUROSCI.0504-11.2011.
45. **Komban SJ**, **Kremkow J**, **Jin J**, **Wang Y**, **Lashgari R**, **Li X**, **Zaidi Q**, **Alonso JM.** Neuronal and perceptual differences in the temporal processing of darks and lights. *Neuron* 82: 224–234, 2014. doi:10.1016/j.neuron.2014.02.020.
46. **Lu ZL**, **Sperling G.** Black-white asymmetry in visual perception. *J Vis* 12: 8, 2012. doi:10.1167/12.10.8.
47. **Bellet ME**, **Bellet J**, **Nienborg H**, **Hafed ZM**, **Berens P.** Human-level saccade detection performance using deep neural networks. *J Neurophysiol* 121: 646–661, 2019. doi:10.1152/jn.00601.2018.
48. **Bellet J**, **Chen CY**, **Hafed ZM.** Sequential hemifield gating of α- and β-behavioral performance oscillations after microsaccades. *J Neurophysiol* 118: 2789–2805, 2017. doi:10.1152/jn.00253.2017.
49. **Maris E**, **Oostenveld R.** Nonparametric statistical testing of EEG- and MEG-data. *J Neurosci Methods* 164: 177–190, 2007. doi:10.1016/j.jneumeth.2007.03.024.
50. **Idrees S**, **Baumann MP**, **Franke F**, **Münch TA**, **Hafed ZM.** Perceptual saccadic suppression starts in the retina. *Nat Commun* 11: 1977, 2020. doi:10.1038/s41467-020-15890-w.
51. **Hubel DH**, **Wiesel TN.** Receptive fields and functional architecture of monkey striate cortex. *J Physiol* 195: 215–243, 1968. doi:10.1113/jphysiol.1968.sp008455.
52. **Knierim JJ**, **Van Essen DC.** Visual cortex: cartography, connectivity, and concurrent processing. *Curr Opin Neurobiol* 2: 150–155, 1992. doi:10.1016/0959-4388(92)90003-4.
53. **Pastukhov A**, **Braun J.** Rare but precious: microsaccades are highly informative about attentional allocation. *Vision Res* 50: 1173–1184, 2010. doi:10.1016/j.visres.2010.04.007.
54. **Buonocore A**, **Baumann MP**, **Hafed ZM.** Visual pattern analysis by motor neurons (Abstract). *Computational and Systems Neuroscience (Cosyne) 2020 Conference*, Denver, CO, February 27–March 1, 2020, p. 147.
55. **Büttner-Ennever JA**, **Cohen B**, **Pause M**, **Fries W.** Raphe nucleus of the pons containing omnipause neurons of the oculomotor system in the monkey, and its homologue in man. *J Comp Neurol* 267: 307–321, 1988. doi:10.1002/cne.902670302.
56. **Everling S**, **Paré M**, **Dorris MC**, **Munoz DP.** Comparison of the discharge characteristics of brain stem omnipause neurons and superior colliculus fixation neurons in monkey: implications for control of fixation and saccade behavior. *J Neurophysiol* 79: 511–528, 1998. doi:10.1152/jn.1998.79.2.511.
57. **Gandhi NJ**, **Keller EL.** Activity of the brain stem omnipause neurons during saccades perturbed by stimulation of the primate superior colliculus. *J Neurophysiol* 82: 3254–3267, 1999. doi:10.1152/jn.1999.82.6.3254.
58. **Buonocore A**, **Purokayastha S**, **McIntosh RD.** Saccade reorienting is facilitated by pausing the oculomotor program. *J Cogn Neurosci* 29: 2068–2080, 2017. doi:10.1162/jocn_a_01179.
59. **Westner BU**, **Dalal SS.** Faster than the brain's speed of light: retinocortical interactions differ in high frequency activity when

processing darks and lights (Preprint). *BioRxiv* 153551, 2019. doi:10.1101/153551.
60. **Jin J**, **Wang Y**, **Lashgari R**, **Swadlow HA**, **Alonso JM.** Faster thalamocortical processing for dark than light visual targets. *J Neurosci* 31: 17471–17479, 2011. doi:10.1523/JNEUROSCI.2456-11.2011.
61. **Jin JZ**, **Weng C**, **Yeh CI**, **Gordon JA**, **Ruthazer ES**, **Stryker MP**, **Swadlow HA**, **Alonso JM.** On and off domains of geniculate afferents in cat primary visual cortex. *Nat Neurosci* 11: 88–94, 2008. doi:10.1038/nn2029.
62. **Klein RM.** Inhibition of return. *Trends Cogn Sci* 4: 138–147, 2000. doi:10.1016/S1364-6613(00)01452-2.
63. **Posner MI.** Orienting of attention. *Q J Exp Psychol* 32: 3–25, 1980. doi:10.1080/00335558008248231.
64. **Posner MI**, **Cohen Y.** Components of visual orienting. In: *Attention and Performance X*, edited by Bouma H, Bowhuis D. Hillsdale, NJ: Erlbaum, 1984, p. 531–556.
65. **Mele S**, **Savazzi S**, **Marzi CA**, **Berlucchi G.** Reaction time inhibition from subliminal cues: is it related to inhibition of return? *Neuropsychologia* 46: 810–819, 2008. doi:10.1016/j.neuropsychologia.2007.11.003.
66. **Wright RD**, **Richard CM.** Sensory mediation of stimulus-driven attentional capture in multiple-cue displays. *Percept Psychophys* 65: 925–938, 2003. doi:10.3758/BF03194824.
67. **Zhao Y**, **Heinke D.** What causes IOR? Attention or perception? — manipulating cue and target luminance in either blocked or mixed condition. *Vision Res* 105: 37–46, 2014. doi:10.1016/j.visres.2014.08.020.